International Journal of Heat and Technology
Vol. 40, No. 4, August, 2022, pp. 976-986
Journal homepage: http://iieta.org/journals/ijht

Modeling and Simulation of Hourly Irradiance for Solar Applications in Chad: Case of the City of Abeche

Ahmed Ismaël Arim[1], Mahamat Hassane Babikir[1,2], Venant Sorel Chara-Dackou[1*], Donatien Njomo[1]

[1] Environmental Energy Technologies Laboratory (EETL), Department of Physics, Faculty of Science, University of Yaounde 1, P.O. Box 812, Yaounde, Cameroon
[2] Department of Physics, University of Ndjamena, P.O Box 1117, Chad

Corresponding Author Email: chav7@yahoo.com

https://doi.org/10.18280/ijht.400415

Received: 1 June 2022
Accepted: 12 August 2022

Keywords:
modeling and simulation, solar energy, hourly irradiance, solar applications, climate region

ABSTRACT

In this paper, the general objective is to model and simulate the hourly irradiance followed by an assessment of the solar potential in the city of Abeche located in the climatic region of the Republic of Chad. Unlike previous work carried out in the study area on solar irradiance, two hourly solar irradiance estimation models (Capderou and Liu&Jordan) were simulated at varying tilt angles. An analysis of the quality of their estimation is carried out through statistical methods (MBD, RMSD, MAD) of error calculation. The results show that the first model is well adapted on a horizontal surface to estimate the solar radiation and also during the dry season when the surface is inclined. On the other hand, the second model is preferred during the rainy season when the surface is inclined. The solar energy over the entire area of Abeche is estimated at 427 GWh on a horizontal surface in January and 504 GWh for the month of August on a tilted surface. This can be exploited by all solar technologies or applications.

1. INTRODUCTION

The development of scientific research in recent years has led to many discoveries, proposing more efficient technological solutions in several branches of production of goods and services (agricultural, industrial, etc...). These technologies sometimes require decentralized energy production systems. Thus, the need for energy is becoming more and more important. Chad is one of the Sahelian countries that, thanks to its geographical position, has a very high renewable energy potential, particularly wind and solar energy, which unfortunately are not used to cover the population's energy needs [1-6]. The city of Abeche covers an area of 3,000 hectares and is located in the Sahelian climatic zone in eastern Chad (Figure 1), with geographical coordinates of 13°85 North and 20°85 East and an altitude of 545 meters. It is located in a geologically contrasted area with plains, plateaus and small mountain ranges. This city is one of the regions of Chad where the daily sunshine duration is about 8 hours and the global radiation on a horizontal plane is estimated at more than 5 kWh/m^2.day [7]. In spite of this, its electricity coverage rate is very low and it has a very difficult water supply in its localities. The increasing demand for solar energy is focusing all attention on solar solutions [8]. Thanks to the considerable advances in scientific research in the field of solar energy [9], innovative results are offered to the solar industries in order to propose more effective and efficient solutions in all their production branches [10]. However, local applicability can only be well realized when all the necessary information about the existing solar potential and resources is known, available and can be easily obtained through accessible tools [10-12]. In this context, scientific efforts have been made in order to propose methods [13], tools and techniques that can be used to assess the solar resources in the regions of the earth's surface [14, 15]. The knowledge of the climate and its seasonal variability in a given region is an indispensable capacity factor in the process of evaluating its solar resources in order to find an adequate tool for quantification [16, 17]. Thus, investigators in the literature multiply studies on solar radiation modeling using several processes to evaluate the solar potential [18]. The estimation of solar radiation can be done on a monthly, daily or hourly basis and the radiation models are chosen according to the type of resolution required and also with respect to the availability of the necessary data as input to the model. In general, in the case of daily and monthly solar radiation estimates, empirical models that on the one hand use sunshine duration measurements and on the other hand do not use sunshine duration measurements [19], techniques based on the use of artificial neural network [20], long-term daily global radiation estimation models [21] and many other techniques [22-24] are useful. In the case of hourly estimation of solar radiation, radiation prediction models [25] and estimation models often called semi-empirical models [4, 26, 27], are the models used in previous works in the literature. Studies have been carried out to evaluate the solar potential in the city of Abeche with the aim of developing solar energy as a source of energy that is not only abundant and free but also environmentally friendly. Babikir et al. [28] evaluated the potential of hourly global solar radiation in five cities in Chad, including Abeche, by proposing a solar radiation estimation model. However, the diffuse and direct components of solar radiation are not evaluated, yet the knowledge of the values of these components is important for the choice of the different solar technology systems that can be used and also the orientation of the collection surface to optimize the collection of incident

radiation. Souloukngа et al. [7] have proposed empirical models to evaluate the daily global solar radiation on the ground on a horizontal plane in the Sahelian climatic region. These models estimate more the global radiation on horizontal surfaces and require the knowledge of several input parameters (sunshine duration, pressure, humidity, temperature). This not only makes the use of the model difficult but also does not give enough information about the solar potential in the city as a whole. It is therefore necessary to use estimation models called semi-empirical models, which require reliable data on the geographical coordinates of the study area.

The objective of this study is to model and simulate the hourly irradiance and then to evaluate the daily hourly solar radiation potential on different planes with respect to the ground from an estimation model satisfying the climatic conditions in the city of Abeche at variable angles of inclination (horizontal and tilted) of the sensor with respect to the ground. In this work, the Capderou model and the Liu&Jordan model are chosen to estimate the hourly solar potential in the city of Abeche. This choice is motivated by the reasons provided above and the limitations of the models proposed to evaluate the solar radiation in this city. In addition, in the literature these models are much more appreciated for their estimation qualities on different planes of capture and their ease of use when only the data of the geographical coordinates of the locality are known with certainty and available [4, 29, 30]. In a first step, both models will be used to evaluate the global irradiance on a horizontal plane and the values of their estimates will be compared to the data from the SoDa-HelioClim-3 database used as reference data (or measured data) in this work. Statistical techniques for error evaluation will be used to assess the models on a monthly and annual basis. After the validation of the best model, it will be useful to estimate all components of solar irradiance (global, direct and diffuse) on a horizontal ground plane. In the second step, the same procedure will be repeated in the case of a surface inclined to the ground, until the evaluation of the hourly solar potential. In both cases of studies carried out, the validation of the models is made on the global component of the solar radiation.

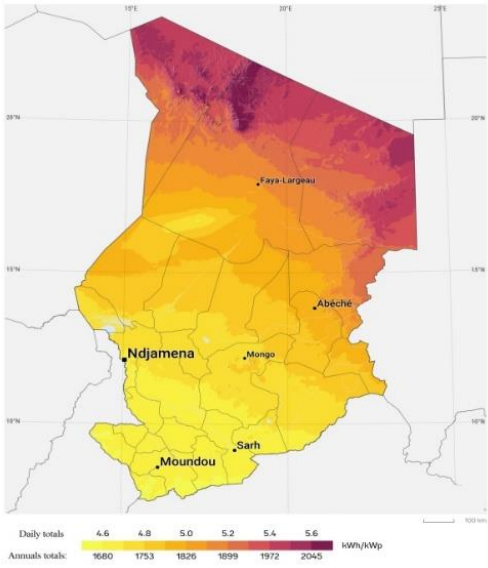

Figure 1. Map of solar potential in Chad. It is the potential of the global solar radiation on horizontal plane (published by World Group Bank, ESMAP, https://globalsolaratlas.info)

2. MATHEMATICAL MODEL

2.1 Astronomical parameters

The position of the sun in the sky can be well known at any time of the day by the knowledge of parameters like solar declination, hour angle and sun height and sun azimuth [16]. From there, some astronomical parameters like the extra-atmospheric radiation, the true solar time (TSV) and the equation of time (ET) can be calculated. Their determination is essential in the development of mathematical models of solar radiation. The relation to calculate the height of the sun is given by the Eq. (1) [16]:

$$\sin(h) = \left[\cos(d)\cos(\phi)\cos(\Omega) + \sin(\phi)\sin(d)\right] \quad (1)$$

Solar declination d can be determined from the Eq. (2)

$$d = \arcsin\left[0.369\sin\left(\frac{360}{365}(j-82) + 2\sin\left((j-2)\frac{360}{365}\right)\right)\right] \quad (2)$$

With j Klein's number of days [18], and ϕ the latitude of the study area expressed in degrees.

The hour angle Ω is calculated using the following relation [11]:

$$\Omega = 15(TSV - 12) \quad (3)$$

By using the true solar time (TSV) obtained from the Eq. (4):

$$TSV = TL - DE - \frac{\lambda}{15} + ET \quad (4)$$

where, λ is the longitude of the study area, TL the local time and ET equation of time obtained by Eq. (5):

$$ET = 9.87\sin(2\eta) - 7.35\eta - 1.5\sin(\eta) \quad (5)$$

With

$$\eta = \frac{360}{365}(j-81), DE = 1 \quad (6)$$

2.2 Capderou model

The mathematical formulation of this model takes into account the two types of surface depending on whether relation to the ground [4].

2.2.1 Horizontal plane estimation model

Linke's disorder factor. As it passes through the atmosphere solar radiation undergoes several phenomena such as scattering absorption and emission through air molecules, particles in the atmosphere, aerosols. These aspects are taken into account in the mathematical formulation of the Linke's disorder factor. This is subdivided into three sub-factors taking into account the different atmospheric disturbances. It is noted Tl and calculated by the relation:

$$Tl = T_1 + T_2 + T_0 \quad (7)$$

The disorder due to gas absorption T_0 is calculated from Eq. (8):

$$T_0 = 2.4\text{-}0.9\sin(\phi) + 0.1\text{Ahe}(2+\sin(\phi)) \\ -0.2\text{z-}(1.22+0.14\text{Ahe})(1\text{-}\sin(\text{h})) \quad (8)$$

With the winter-summer alternation *Ahe* given by the expression (9):

$$Ahe = \sin\left(\frac{360}{365}(\text{j-}121)\right) \quad (9)$$

The aerosol diffusion disorder is a function of the winter-summer alternation noted T_2. It is calculated from Eq. (10):

$$T_2 = (0.9 + 0.4Ahe)(0.63)^{\text{Z}} \quad (10)$$

where, z is the altitude of the location expressed in kilometers. The disorder due to the absorption noted T_1 by gases (O_2, CO_2 and O_3) and to the molecular diffusion of Rayleigh is obtained from the expression (11):

$$T_1 = (0.89)^{\text{Z}} \quad (11)$$

Beam radiation. The first component of solar radiation is calculated from the following expression.

$$I_{D,H} = I_{nor}\sin(\text{h}) \quad (12)$$

where, the normal incident solar radiation can be obtained by the relation (13):

$$I_{nor} = I_S \exp\left[-Tl\left(0.9 + \frac{9.4\sin(\text{h})}{0.89^{\text{Z}}}\right)^{-1}\right] \quad (13)$$

I_S a function whose expression is as follows:

$$I_S = I_0\left[1 + 0.033\cos\left(\frac{360}{365}(j-2)\right)\right] \quad (14)$$

I_0=1367W/m^2 is the solar constant.

Diffuse radiation. The diffuse solar radiation on a horizontal plane per sky is given by the expression (15):

$$I_{d,H} = I_S \exp\left(-1 + 1.06\ln(\sin(h)) + a_1 - \sqrt{a_1^{\,2} + b_1^{\,2}}\right) \quad (15)$$

With,

$$b_1 = \log(Tl - T_0) - 2.8 + 1.02(1 - \sin(h))^2 \\ \text{And } a_1 = 1.1 \quad (16)$$

Thus, the global component can be deduced and given by:

$$I_{G,H} = I_{D,H} + I_{d,H} \quad (17)$$

2.2.2 Estimation model on an inclined plane

The inclination of the receiving surface of the incident solar flux is an optimal system in the collection of the solar flux. This allows the receiving surface to receive more of the normal incident flux and other diffuse radiation from the sky, thus increasing the overall component.

Beam radiation. The direct component is determined by the relationship:

$$I_{D,I} = I_{nor}\cos(i) \quad (18)$$

This expression depends on the angle of incidence *i* which is determined from the equation:

$$\cos(i) = \sin(\alpha)\sin(\Omega)\cos(\gamma)\cos(d) \\ + \cos(\alpha)\cos(\gamma)\left[\cos(\Omega)\cos(d)\sin(\phi) - \sin(d)\cos(\phi)\right] \quad (19) \\ + \sin(\gamma)\cos(\Omega)\cos(d)\cos(\phi) + \sin(d)\sin(\phi)$$

With

$$\gamma = \frac{\pi}{2} - \beta \quad (20)$$

When the receiving surface is facing south, the angle α is zero. The angle that the receiving surface makes with the horizontal when it is tilted is β. It varies according to the cases studied.

Diffuse radiation. The diffuse component received on a tilted surface is composed of the diffuse irradiance from the ground, the sky and the backscattered diffuse irradiance. This can be formulated mathematically as follows:

$$I_{d,I} = I_{d,sky} + I_{d,ground} + I_r \quad (21)$$

The first component is the fraction of solar radiation diffused by the sky when it receives the incident solar flux. It is calculated by the following relation (Eq. (22)).

$$I_{d,sky} = \Gamma_1\cos(i) + (1 + \sin(\gamma))\frac{\Gamma_2}{2} + \Gamma_3\cos(\gamma) \\ with \\ a = 3.1 - 0.4b \quad (22) \\ b = \ln(T_1 - T_0) - 2.28 - 0.5\ln[\sin(h)]$$

$$\Gamma_1 = I_S \exp\left[-2.48 + \sin(h) + a - (a^2 + b^2)^{1/2}\right] \quad (23)$$

The isotropic component for a sky of uniform luminance:

$$\Gamma_2 = I_{d,H} - \Gamma_1\sin(h) \quad (24)$$

The horizon circle component:

$$\Gamma_3 = I_S\left(\frac{-0.02}{a_2^{\,2} + a_2 b_2 + 1.8}\right)\exp[\sin(h)] \\ with \\ b_2 = \exp(0.2 + 1.75\ln(\sin(h))) \quad (25) \\ a_2 = \ln(T_1 - T_0) - 3.1 - \ln(\sin(h))$$

The second component of the diffuse radiation on a tilted surface, coming from the ground, is determined from Eq. (26), a function of the albedo.

$$I_{d,ground} = \rho I_{G,H} \frac{1-\sin(\gamma)}{2} \tag{26}$$

The diffused backscattered irradiance which is the third component is calculated from the equation:

$$I_r = 0.9(\rho - 0.2) I_{G,H} \exp\left(-\frac{4}{\sqrt{T_1 - T_0}}\right) \tag{27}$$

From expressions (18) and (21), the global radiation on a tilted surface can be deduced.

2.3 Liu&Jordan model

Like the Capderou model, it takes into account in its mathematical formulation the quantification of the flux incident on different surfaces (horizontal and tilted). This model is very popular in the literature in practice when the estimation of solar radiation is made on a tilted surface of any angle from the horizontal [28].

2.3.1 Model of estimation on horizontal plane

Beam radiation. The relationship to calculate its direct component on the ground on a horizontal plane is written as:

$$I_{D,H} = \varphi_1 \sin(h) \exp\left(\frac{-1}{\varphi_2 \sin(h+2)}\right) \tag{28}$$

where, the parameters φ_1 and φ_2 are chosen according to the state of the atmosphere from Table 1.

Table 1. Values of the parameters

State of the sky	φ_1	Φ_3	φ_2
Clear sky	1300	87	6
Medium sky	1230	125	4
Cloudy sky	1200	187	5

Diffuse radiation. Thus, the diffuse component of solar radiation is calculated from the relationship function of the height of the sun in the sky and the parameter representing the state of the sky:

$$I_{d,H} = \varphi_3 \left[\sin(h)\right]^{0.4} \tag{29}$$

2.3.2 Estimation model on an inclined plane

Beam radiation. The calculation of the direct component of solar radiation for this type of surface is made from the following relationship:

$$I_{D,I} = \left(I_{G,H} - I_{d,H}\right) \frac{\cos(i)}{\cos(i_Z)} \tag{30}$$

i_z is the zenith angle. It is related to the height by the relation (31):

$$i_Z = \frac{\pi}{2} - h \tag{31}$$

The Diffuse component is obtained by using the following relationship:

$$I_{d,I} = I_{sky} + I_{re} \tag{32}$$

The first component is the incident flux received by the sky and is diffused. The relation that allows to calculate it is:

$$I_{sky} = I_{d,H} \frac{1+\cos(\beta)}{2} \tag{33}$$

The second is the Diffuse Solar Flux coming from the reflection on the ground of the global solar flux. It is obtained from Eq. (34):

$$I_{re} = \rho\left(I_{D,H} + I_{d,H}\right) \frac{1+\cos(\beta)}{2} \tag{34}$$

The sum of Eq. (30) and (32) gives the global component.

2.4 Statistical evaluation methods

The statistical indicators of error calculation are used to measure the performance of the models. This makes it possible to compare them and to choose the one most adapted to the climatic variability of the study area. The indicators chosen are the mean bias deviation (MBD), the mean absolute deviation (MAD) and the root mean square deviation (RMSD) [11]. These are relative errors expressed in terms of percentage and calculated from the following relationships:

$$MBD = \frac{1}{n} \sum_{i=1}^{n} \frac{I_{e,i} - I_{m,i}}{I_{m,i}} \tag{35}$$

$$MAD = \frac{1}{n} \sum_{i=1}^{n} \left| \frac{I_{e,i} - I_{m,i}}{I_{m,i}} \right| \tag{36}$$

$$RMSD = \sqrt{\frac{1}{n} \sum_{i=1}^{n} \left(\frac{I_{e,i} - I_{m,i}}{I_{m,i}} \right)^2} \tag{37}$$

where, n is the number of observations, e means estimated and m means measured.

3. RESULTS AND DISCUSSIONS

In this section, the solar radiation is evaluated over an assumed horizontal surface with respect to the ground. In Figure 2, the monthly variations of the hourly global irradiance estimated by the models are simulated and observed. For each month of the year, the hourly evolution during a day is compared to the HelioClim-3 data (named on the figures "data"). During the months of December, January and February, the estimated global radiation values are all close, with a very small difference observed between 6am and 9am and 3pm and 6pm showing a strong positive correlation

between the models. Compared to the measured data, between 6am and 9am both models tend to underestimate the global radiation and overestimate it between 12pm and 6pm. These differences from noon to sunset become more and more important and go up progressively during the following months until the sunrise in August, before tightening slowly until the end of autumn to reach 11h during a day. Over the whole months, from noon onwards, both models have difficulty in approaching the measured values, which makes it appear that the estimates are better than between sunrise and noon.

3.1 Evaluation of solar radiation on a horizontal plane on the ground

In this section, the solar radiation is evaluated on an assumed horizontal surface with respect to the ground. In Figure 2, the monthly variations of the hourly global irradiance estimated by the models are simulated and observed. For each month of the year, the hourly evolution during a day is compared to the HelioClim-3 data (named on the figures "data"). During the months of December, January and February, the estimated global radiation values are all very well correlated, with a very small difference observed between 6am and 9am and 3pm and 6pm showing a strong positive correlation between the models. Compared to the measured data, between 6am and 9am both models tend to underestimate the global radiation and overestimate it between 12pm and 6pm. These differences from noon to sunset become more and more important and go up progressively during the following months until the sunrise in August, before tightening slowly until the end of autumn to reach 11 hours during a day. Over the whole months, from noon onwards, both models have difficulty in approaching the measured values, which makes it appear that the estimates are better than between sunrise and noon.

These observed deviations, which are the results of over- and under-estimations, may be due to the fact that the models used are deterministic and that there is no term in the mathematical formulation that takes into account some meteorological phenomena, unobserved atmospheric disturbances such as water vapor and others that influence the radiation incident on the passage of the atmosphere. In other words, it could be said that some specificities of the climate in the city would not be taken into account by variables in the models or they would not be well taken into account. In addition, the shadows due to the city's relief, which influence the solar power received on the ground, would not be taken into account. The two models show a good agreement with the data measured from the calculation of the correlation coefficient (Capderou R = 0.966 and Liu&Jordan R = 0.953) and the results presented in Figure 3 for the Capderou model and Figure 4 for the Liu&Jordan model.

On the whole of all the months, the Capderou model is better fitted than the Liu&Jordan model referring to the results of comparison of the errors calculated in the estimates of the global radiation values by the different models on a horizontal surface in Figure 12 where the three error calculations validate the model and also of the results of Figure 5 describing the differences between the daily averages taken over a month of the irradiation values. Table 2, in a general way from the average of MAD, MBD and RMSD validates the Capderou model as the best adapted to estimate the global solar radiation on a horizontal surface in this city.

Table 2. Comparison of statistical results of the errors of the global irradiance estimates on horizontal plane of the two simulated models in percent (%)

	MBD	MAD	RMSD
Capderou	12.9	12.9	16
Liu&Jordan	23.7	23.7	28.5

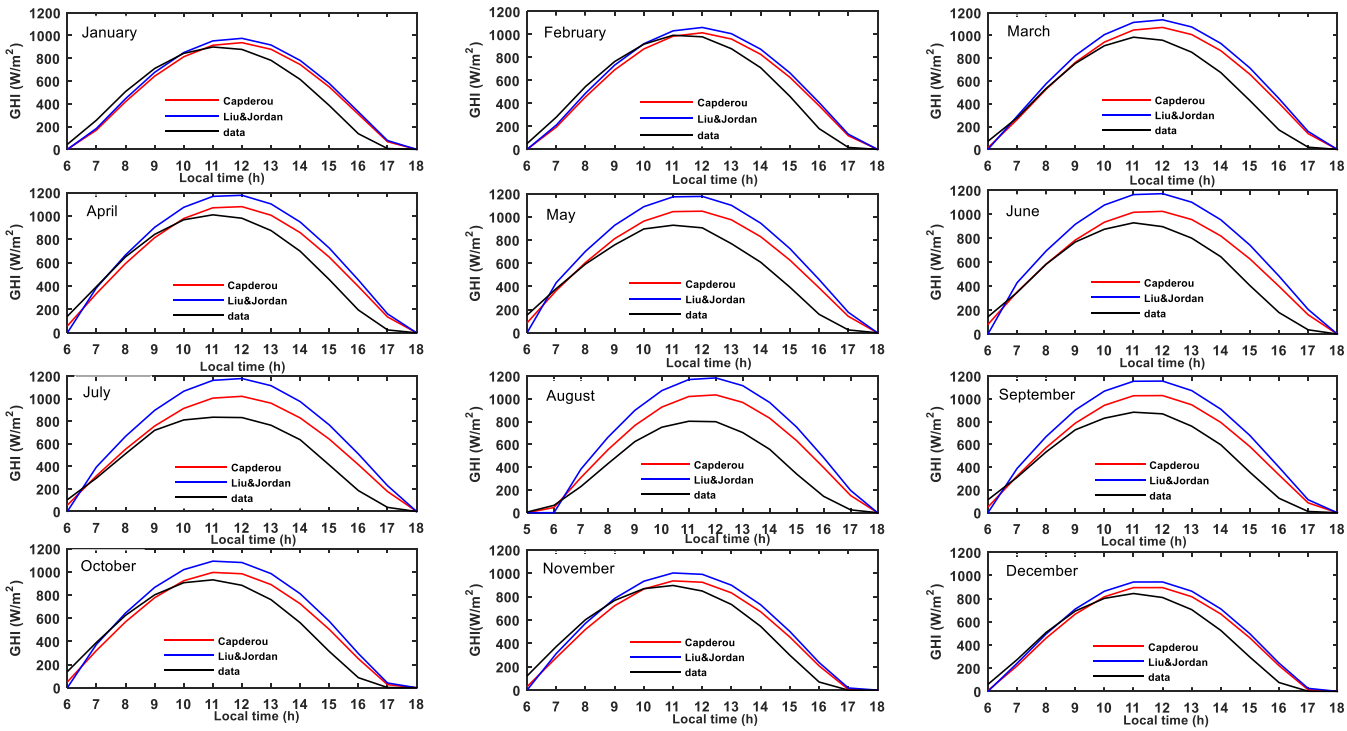

Figure 2. Comparison between monthly evolutions of hourly global irradiance estimated by the models and the data measured on a horizontal plane

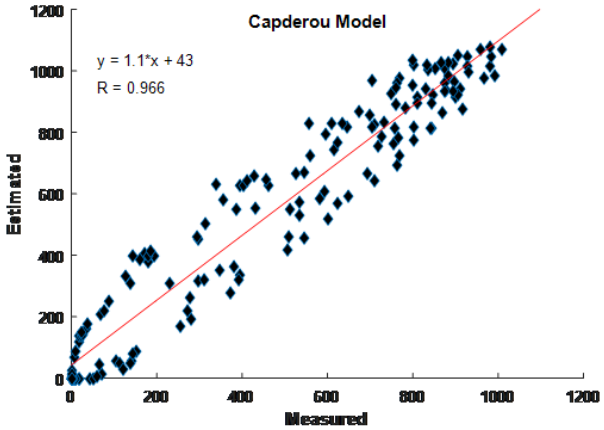

Figure 3. Linear relationship between the measured values and the values predicted by the Capderou model for a horizontal ground plane. R is the linear correlation coefficient and the equation y=ax+b is the linear regression model

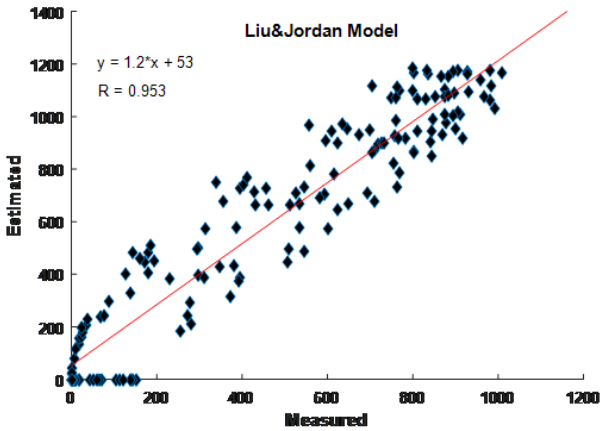

Figure 4. Linear relationship between the measured values and the values predicted by the Liu&Jordan model for a horizontal ground plane. R is the linear correlation coefficient and the equation y=ax+b is the linear regression model

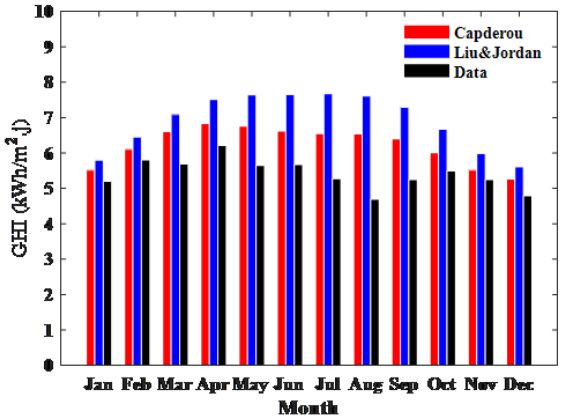

Figure 5. Comparison between the monthly average values of daily global irradiation estimated by the two models and those measured on a horizontal surface

After validation of the estimation model, all the solar radiation components on a horizontal plane are simulated and their daily evolution during every month is described in Figure 6. Thus, their hourly variability can be evaluated giving rise to an estimate of solar energy that can be exploited each hour of the day for conversion into either thermal or electrical energy. The direct component grows strongly during the day and reaches an average of 350 W/m^2 at 8 am and is around 400 W/m^2 at 3 pm. The maximum value reached is on average 800W/m^2 around noon. This can heat fluids up to high temperatures that can be used and also make the photovoltaic panels work optimally. Thus, during each hour of the day in January, the solar energy received is estimated to be 410 Wh/m^2 or 12710 Wh/m^2 the whole month. This can be estimated at 381 GWh for the entire city area. For the global radiation, the flux received each hour of the day in January is estimated at 14260 Wh/m^2 or 427 GWh for the whole month. This potential shows that photovoltaic and thermodynamic solar technologies can be installed and used in the climatic conditions of the city of Abeche.

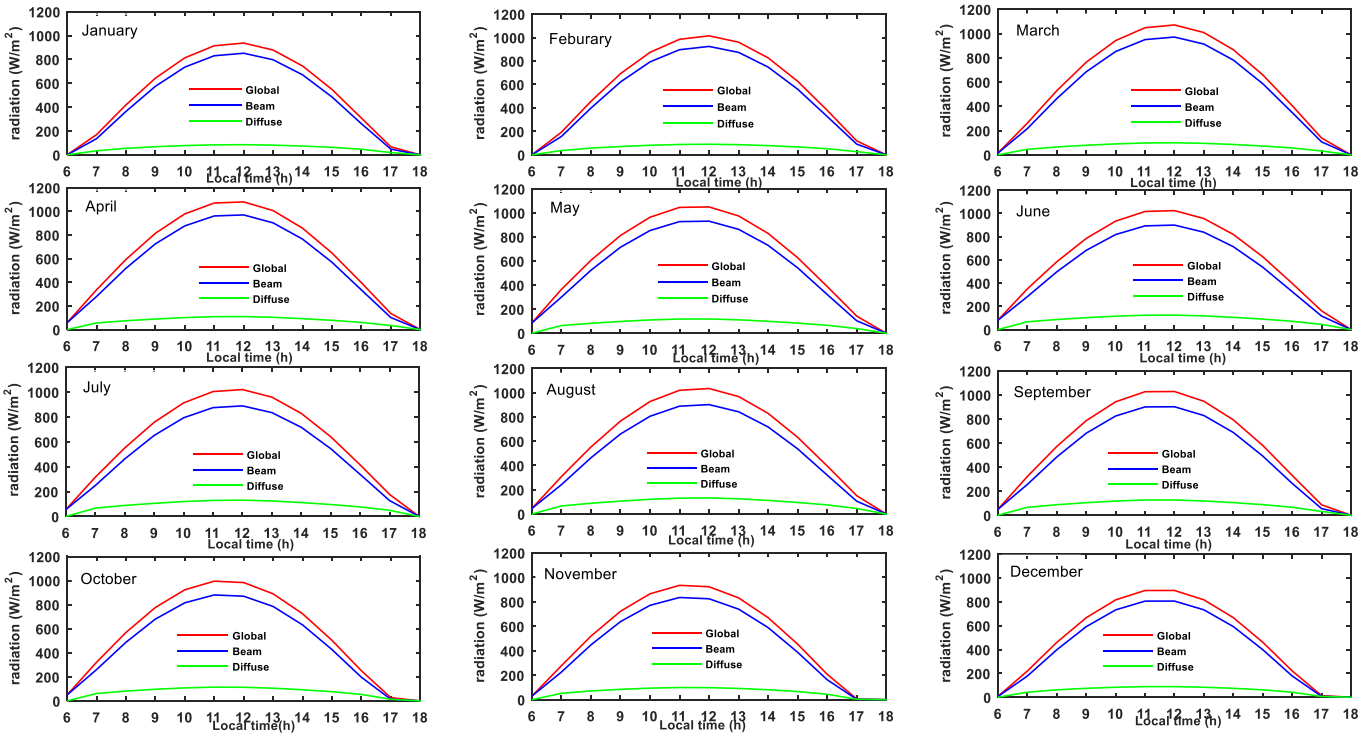

Figure 6. Monthly evaluation of hourly solar irradiance components on a horizontal plane by the Capderou model

3.2 Evaluation of solar radiation on a plane inclined to the ground

In this second section, solar radiation is evaluated on a surface tilted at an angle of 15° from the horizontal and oriented to the south. The global solar radiation is estimated by both models and the estimated values are compared with those of the measured data in Figure 7. The two models are strongly correlated during the days of February, March, September and October. Compared to the measured data the models as in the case of a horizontal surface, before noon are slightly more approaching the ideal and afterwards overestimate the solar radiation values until sunset. This is true for all months of the year. It can be seen that from the middle of autumn to the end of winter (the so-called arid season), the Capderou model gives good and significant results where the calculated errors on average do not exceed 20% (Figure 12), while during the other months or periods (the so-called pluvial season), the Liu&Jordan model presents the most minimal errors. In general, the estimated values of radiation by both models are well correlated with the measured data (Capderou R = 0.947 and Liu&Jordan R = 0.965). There is a linear relationship between them i.e. the estimated values can be explained by the measured values. This is described in Figure 8 and Figure 9.

It can be seen that between the months of May and September the errors are significant, reaching about 60%. This is due to the fact that during this period, the sky is on average covered. The model of Liu & Jordan has taken into account the different states of the sky from the fixed parameters (constants), while when the sky is for example covered; the cloudiness varies from one month to another and the same for a clear sky. In Capderou's model, we notice that the state of the sky has been implicitly taken into account via the incident diffuse irradiance from the sky, so this could be due to a bad specification in that the radiation on an inclined plane depends on that on a horizontal plane. This reasoning can be supported by the results in Figure 12 showing the limitations of the model during overcast periods in the case of a tilted surface. It can therefore be said that the analyses made in the case of solar radiation on a horizontal plane are valid in the case of a tilted plane for both models. According to the climatological table of the locality, the cloudiest period of the year begins in April and ends in October. This would explain the high values of the errors calculated during these periods (Figure 12). The month with the highest cloudiness is August, which explains the maximum error observed (according to the three error calculations) in this month (Figure 12). We can see that during periods of clear skies (very low or insignificant cloud cover) the Capderou model has minor errors and therefore better estimates of solar radiation (Figure 9). On the other hand, during periods of overcast skies (high cloudiness) the Liu&Jordan model has minor errors and therefore better estimates of solar radiation (Figure 10). An annual evaluation of the errors of the two models was made and the results are presented in Table 3. They indicate that the Liu&Jordan model, on annual average, is better than the Capderou model on a tilted surface.

The results obtained in Figure 10 support the analysis in Figure 12 and the described adaptability of the models to the existing climatic seasons (arid and pluvial seasons) in the city of Abeche.

After the validation of the model, all components of solar radiation are then simulated. From Figure 11, the solar energy received each hour of a day can be evaluated. The evaluation of the hourly potential of the direct component makes it possible to project the hourly operation of solar thermodynamic systems. The tilt of the receiving surface increases the diffuse and direct components. The direct component increases significantly at sunrise and reaches a maximum value of 800 W/m^2 (Figure 11). This hourly distribution is well favorable for solar systems using thermodynamic processes when they do not have a solar tracking system and also the photovoltaic system.

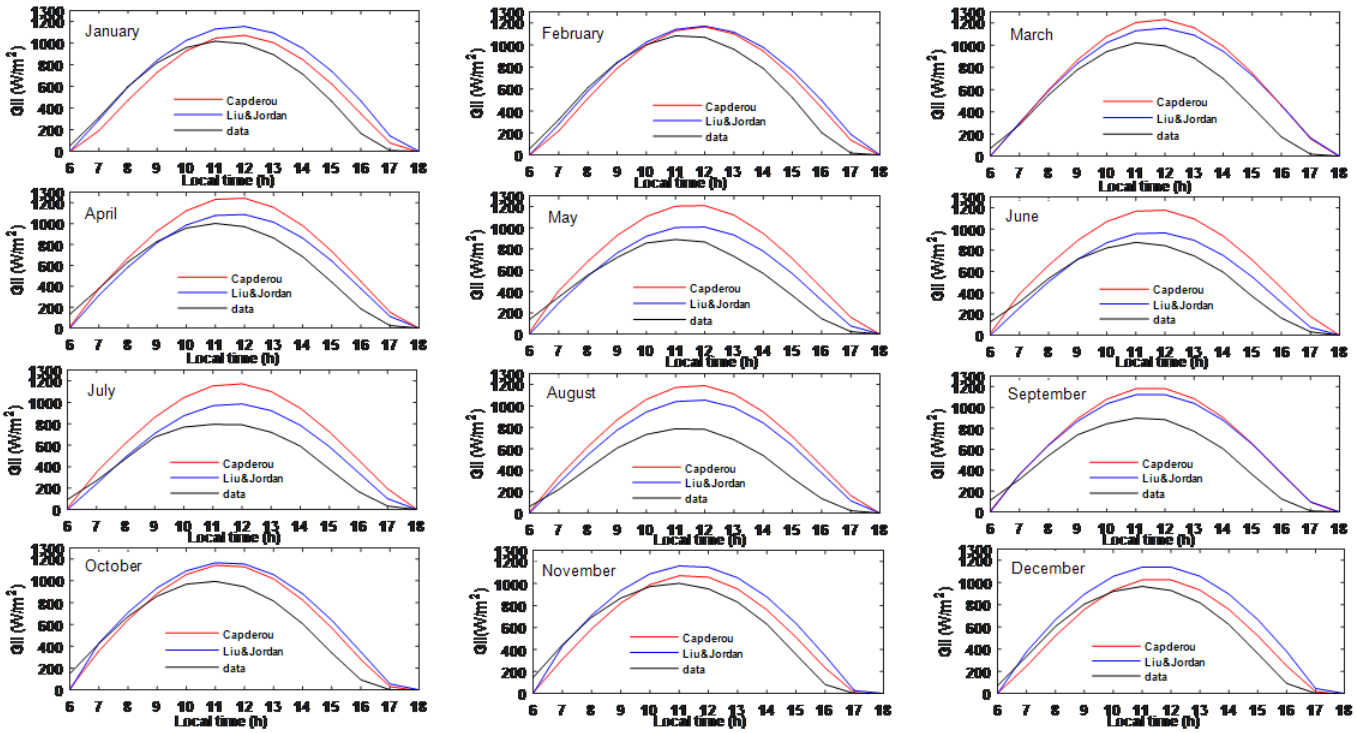

Figure 7. Comparison between the monthly evolution of the hourly global irradiance estimated by the models and the data measured on an inclined plane

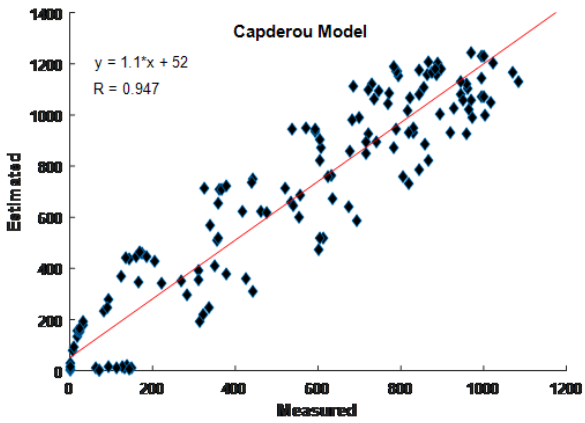

Figure 8. Linear relationship between the measured values and the values predicted by the Capderou model for an inclined plane on the ground. R is the linear correlation coefficient and the equation y=ax+b is the linear regression model

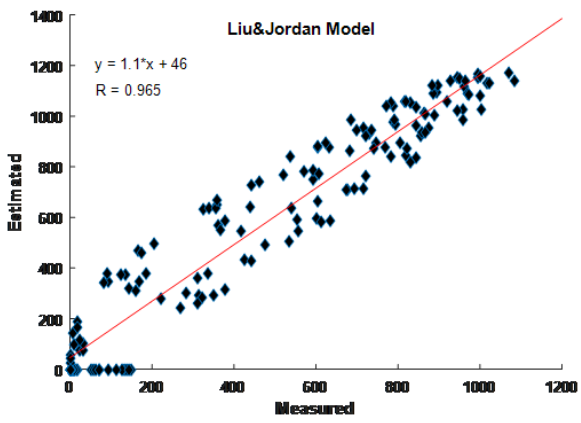

Figure 9. Linear relationship between the measured values and the values predicted by the Capderou model for an inclined plane on the ground. R is the linear correlation coefficient and the equation y=ax+b is the linear regression model

Table 3. Comparison of statistical results of the deviations of the global irradiance estimates on inclined plane of the two simulated models in percent (%)

	MBD	MAD	RMSD
Capderou	22.2	22.2	28.2
Liu&Jordan	18.4	18.4	20.9

During all the days of the year, at 8 am the value of the direct component reaches an average of 400 W/m^2 and turns to about 400 W/m^2 at 3 pm. The maximum value reached is on average 800W/m^2 between 11am and 12pm. This can heat up fluids to high temperatures that can be used and also make the photovoltaic panels work optimally. Thus, during each hour of the day in June, the solar energy received is estimated to be 479 Wh/m^2 or 14849 Wh/m^2 the whole month. This can be estimated at 445 GWh for the whole city area. For the global radiation, the flux received each hour of the day in January is estimated at 16802 Wh/m^2 or 504 GWh for the whole month. This approximates the total electricity production of Chad estimated at about 480 GWh in 2016. This potential shows that solar photovoltaic and thermodynamic technologies can be installed and used in the climatic conditions of the city of Abeche.

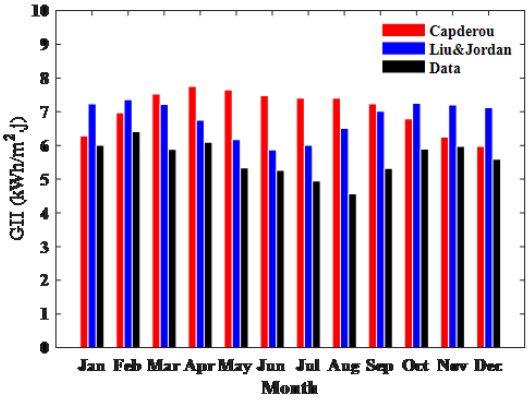

Figure 10. Comparison between the monthly average values of daily global irradiation estimated by the two models and those measured on a tilted surface

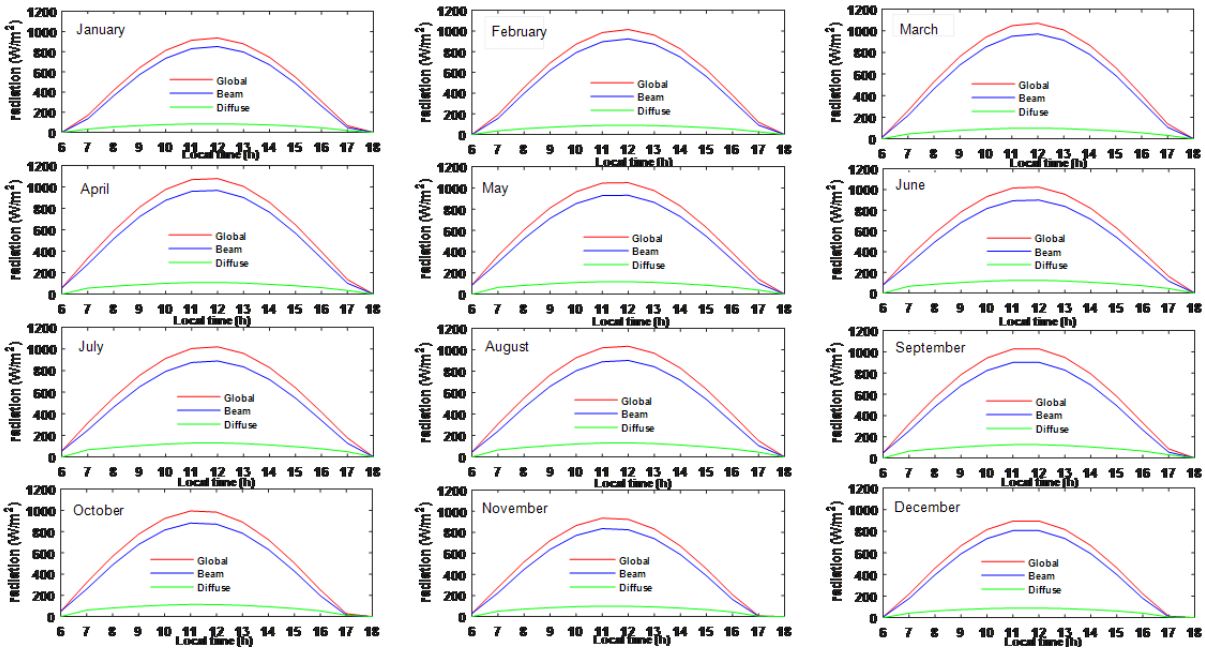

Figure 11. Monthly evaluation of hourly solar irradiance components on an inclined plane by the Liu&Jordan model

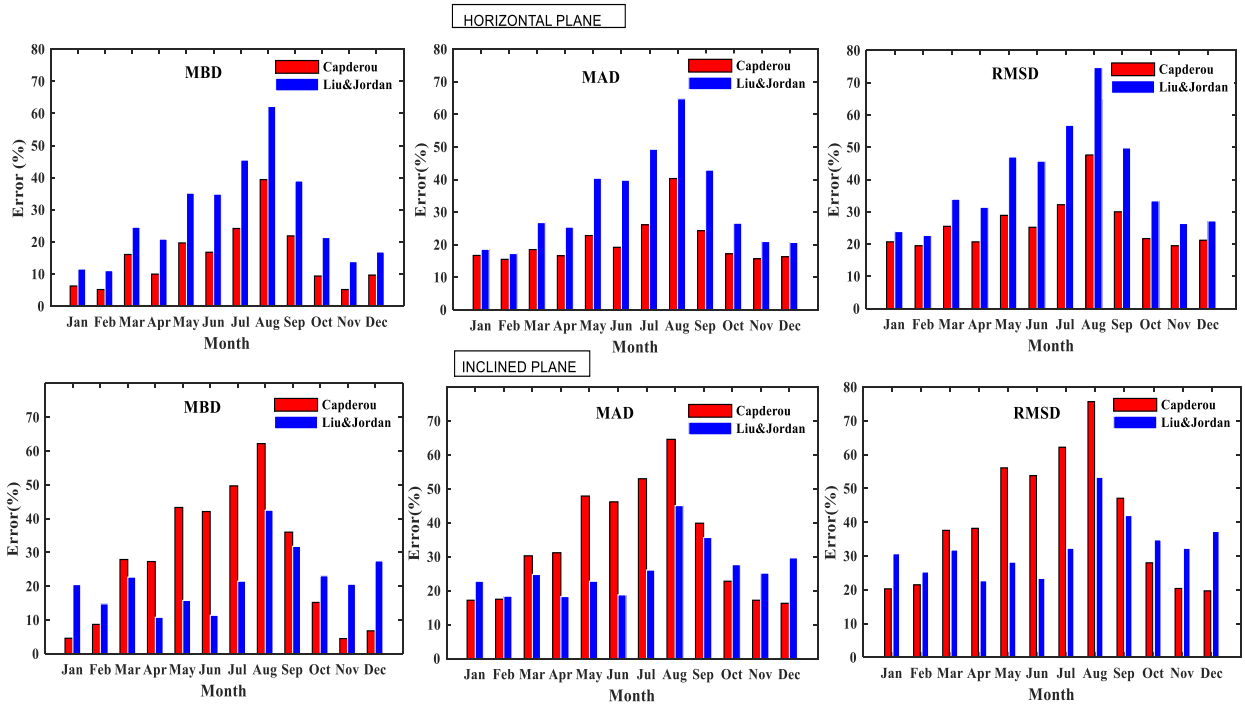

Figure 12. Comparison of the calculated deviations in the estimates of the global radiation values by the different models on horizontal and tilted surfaces

4. CONCLUSIONS

The comparative study carried out in this work has allowed us to propose a model that allows us to evaluate the hourly potential of daily solar radiation. The models simulated in this work are for a clear sky condition and we found through statistical analysis their limitation during periods of high cloudiness at different angles of capture. Nevertheless, the quality of the hourly irradiance estimate over all the days of the months of the year is appreciable. The different validations have allowed to evaluate the hourly potential of solar radiation on the whole territory of Abeche and to show that it is possible to use all solar applications in this city and to obtain good yields. The use of models based on the calculation of Linke's turbidity factor could allow taking into account the cloudiness of the sky caused by the absorption of solar radiation by water vapor and aerosols and its diffusion by dust, aerosols at the crossing of the atmosphere. This while analyzing the variations of this factor in comparison with the measurements made [31-34]. The estimated hourly solar potential on the different surfaces shows that it is possible to use all solar applications in this city and obtain good yields.

REFERENCES

[1] Soulouknga, M.H., Doka, S.Y., Revanna, N., Djongyang, N., Kofane, T.C. (2018). Analysis of wind speed data and wind energy potential in Faya-Largeau, Chad, using Weibull distribution. Renewable Energy, 121: 1-8. https://doi.org/10.1016/j.renene.2018.01.002

[2] Didane, D.H., Wahab, A.A., Shamsudin, S.S., Rosly, N., Zulkafli, M.F., Mohd, S. (2017). Assessment of wind energy potential in the capital city of Chad, N'Djamena. AIP Conference Proceedings, 1831(1): 02004. https://doi.org/10.1063/1.4981190

[3] Didane, D.H., Rosly, N., Zulkafli, M.F., Shamsudin, S.S. (2017). Evaluation of wind energy potential as a power generation source in Chad. International Journal of Rotating Machinery, 2017: 1-10. https://doi.org/10.1155/2017/3121875

[4] Babikir, M.H., Njomo, D., Barka, M., Khayal, M.Y., Goron, D., Chara-Dackou, V.S., Tefouet, M.T., Kamta Legue, D.R., Gram-shou, J.P., Nzadi, S.E. (2020). Modeling the incident solar radiation of the city of N'Djamena (Chad) by the Capderou method. International Journal of Photoenergy, 2020: 1-10. https://doi.org/10.1155/2020/6292147

[5] Goni, S., Adanno, H.A., Diop, D., Kriga, A., Khayal, M.Y., Nebon, B., Beye, A.C., Niang, S.A.A., Drame, M.S. (2019). Observation and simulation of available solar energy at N'Djamena, Chad. Smart Grid and Renewable Energy, 10(6): 165-178. https://doi.org/10.4236/sgre.2019.106011

[6] Goni, S., Adannou, H.A., Diop, D., Drame, M.S., Tikri, B., Barka, M., Beye, A.C. (2019). Long-term variation of sunshine duration and their inter-action with meteorogical parameters over Chad, Central Africa. Natural Resources, 10(3): 47-58. https://doi.org/10.4236/nr.2019.103004

[7] Soulouknga, M.H., Coulibaly, O., Doka, S.Y., Kofane, T.C. (2017). Evaluation of global solar radiation from meteorological data in the Sahelian zone of Chad. Renewables: Wind, Water, and Solar, 4: 4. https://doi.org/10.1186/s40807-017-0041-0

[8] Babikir, M.H., Chara-Dackou, V.S., Njomo, D., Barka, M., Khayal, M.Y., Kamta Legue, D.R., Gram-Shou, J.P. (2020). Simplified modeling and simulation of electricity production from a dish/stirling system. International Journal of Photoenergy, 2020: 1-14. https://doi.org/10.1155/2020/7398496

[9] Barandji, V.D.B., Pakouzou, B.M., Ramdé, E.W.,

M'boliguipa, J., Saria, M., Zoungrana, M., Zerbo, I. (2021). Modeling the response of an illuminated polysilicon solar cell under the influence of radio waves, a 3D approach. Energy Reports, 7: 2094-2100. https://doi.org/10.1016/j.egyr.2021.04.015

[10] Babikir, M.H., Njomo, D., Barka, M., Chara-Dackou, V.S., Kondji, Y.S., Khayal, M.Y. (2021). Thermal modelling of a parabolic trough collector in a quasi-steady state regime. Journal of Renewable and Sustainable Energy, 13(1): 013703. https://doi.org/10.1063/1.5145272

[11] Chara-Dackou, V.S., Njomo, D., Babikir, M.H., Mbouombouo, I.N., Pofoura Gboulie, S.A., Tchinda, R. (2022). Processing sunshine duration measurements for the assessment of solar radiation in climatic regions of the central African republic. Journal of Solar Energy Engineering, 144(3): 031002. https://doi.org/10.1115/1.4053483

[12] Osinowo, A.A., Okogbue, E.C., Ogungbenro, S.B., Fashanu, O. (2015). Analysis of global solar irradiance over climatic zones in Nigeria for solar energy applications. Journal of Solar Energy, 2015: 1-9. http://dx.doi.org/10.1155/2015/819307

[13] Kaplan, A.G., Kaplan, Y.A. (2020). Developing of the new models in solar radiation estimation with curve fitting based on moving least-squares approximation. Renewable Energy, 146: 2462-2471. https://doi.org/10.1016/j.renene.2019.08.095

[14] Bali, T.B., Chara-Dackou, V.S., Goron, D., Babikir, M.H., Njomo, D. (2022). Empirical relationship between global and diffuse radiation and sunshine duration in Chad: Polynomial regression approach. International Journal of Heat and Technology, 40(1): 121-129. https://doi.org/10.18280/ijht.400114

[15] Suehrcke, H., Bowden, R.S., Hollands, K.G.T. (2013). Relationship between sunshine duration and solar radiation. Solar Energy, 92: 160-171. http://dx.doi.org/10.1016/j.solener.2013.02.026

[16] Njomo, D. (1989). Modélisation des variations mensuelles de l'irradiation solaire reçue au Cameroun. Modeling, Simulation and Control, AMSE Press, 18(1): 39-64. https://jglobal.jst.go.jp/en/detail?JGLOBAL_ID=200902043466383409.

[17] Kouassi, A.P.A., Touré, S., Traoré, D. (2020). Seasonal variability of the solar energy potential of the city of Abidjan: Experimental comparative study of two sunshine measurement techniques. Journal of Solar Energy Engineering, 142(1): 011013. https://doi.org/10.1115/1.4044566

[18] Zhang, J., Zhao, L., Deng, S., Xu, W., Zhang, Y. (2017). A critical review of the models used to estimate solar radiation. Renewable and Sustainable Energy Reviews, 70: 314-329. http://dx.doi.org/10.1016/j.rser.2016.11.124

[19] Kutty, H.A., Masral, M.H., Rajendran, P. (2015). Regression model to predict global solar irradiance in Malaysia. International Journal of Photoenergy, 2015: 1-7. http://dx.doi.org/10.1155/2015/347023

[20] Gao, B., Huang, X., Shi, J., Tai Y., Zhang, J. (2020). Hourly forecasting of solar irradiance based on CEEMDAN and multi-strategy CNN-LSTM neural networks. Renewable Energy, 162: 1665-1683. https://doi.org/10.1016/j.renene.2020.09.141

[21] Zou, L., Lin, A., Wang, L., Xia, X., Gong, W., Zhu, H., Zhao, Z. (2016). Long-term variations of estimated global solar radiation and the influencing factors in Hunan province, China during 1980-2013. Meteorology and Atmospheric Physics, 128: 155-165. https://doi.org/10.1007/s00703-015-0410-4

[22] Guher, A.B., Tasdemir, S., Yaniktepe, B. (2020). Effective estimation of hourly global solar radiation using machine learning algorithms. International Journal of Photoenergy, 2020: 1-26. https://doi.org/10.1155/2020/8843620

[23] Al-Hajj, R., Assi, A., Fouad, M. (2021). Short-term prediction of global solar radiation energy using weather data and machine learning ensembles: A comparative study. Journal of Solar Energy Engineering, 143(5): 051003. https://doi.org/10.1115/1.4049624

[24] Guermoui, M., Gairaa, K., Boland, J., Arrif, T. (2021). A novel hybrid model for solar radiation forecasting using support vector machine and bee colony optimization algorithm: Review and case study. Journal of Solar Energy Engineering, 143(2): 020801. https://doi.org/10.1115/1.4047852

[25] Palmer, D., Koubli, E., Cole, I., Betts, T., Gottschalg, R. (2018). Satellite or ground-based measurements for production of site specific hourly irradiance data: Which is most accurate and where? Solar Energy, 165: 240-255. https://doi.org/10.1016/j.solener.2018.03.029

[26] Benchrifa, M., Tadili, R., Idrissi, A., Essalhi, H., Mechaqrane, A. (2021). Development of new models for the estimation of hourly components of solar radiation: Tests, comparisons, and application for the generation of a solar database in Morocco. International Journal of Photoenergy, 2021: 1-16. https://doi.org/10.1155/2021/8897818

[27] Badescu, V., Gueymard, C.A., Cheval, S., Oprea, C., Baciu, M., Dumitrescu, A., Iacobescu, F., Milos, I., Rada, C. (2013). Accuracy analysis for fifty-four clear-sky solar radiation models using routine hourly global irradiance measurements in Romania. Renewable Energy, 55: 85-103. http://dx.doi.org/10.1016/j.renene.2012.11.037

[28] Babikir, M.H., Njomo, D., Khayal, M.Y., Temene, H.D., Joel, D.T. (2018). Estimation of direct solar radiation of Chad. Energy and Power Engineering, 10: 212-225. https://doi.org/10.4236/epe.2018.105015

[29] El Mghouchi, Y., Choulli, Z., Ajzoul, T., El Bouardi, A. (2015). Prediction of solar radiation flues, case study of Tetuan city in northern Morocco. Physical and Chemical News, 75: 41-48.

[30] Sidibé, M., Soro, D., Fassinou, W.F., Toure, S. (2017). Reconstitution of solar radiation on a site of the littoral in Côte D'ivoire. International Journal of Engineering Research and Technology, 10(1): 19-34.

[31] Chaâbane, M., Medhioub, K. (2004). Determination of Linke turbidity factor from solar radiation measurement in northern Tunisia. Renewable Energy, 29(13): 2065-2076. http://doi.org/10.1016/j.renene.2004.03.002

[32] Diabaté, L., Wald, L. (2004). Linke turbidity factors for several sites in Africa. Solar Energy, 75(2): 111-119. http://doi.org/10.1016/j.solener.2003.07.002

[33] Benkaciali, S., Gairaa, K. (2009). Etude expérimentale du trouble atmosphérique sur le site de Ghardaia. Revue des Energies Renouvelables, 12(4): 649-654.

[34] Marif, Y., Chiba, Y., Belhadj, M.M., Zerrouki, M.,

Benhammou, M. (2018). A clear sky irradiation assessment using a modified Algerian solar atlas model in Adrar city. Energy Reports, 4: 84-90. https://doi.org/10.1016/j.egyr.2017.09.002

NOMENCLATURE

TSV	true solar time, hour
ET	Equation of time, hour
TL	Local time, hour
MBD	Mean bias deviation, %
MAD	Mean absolute deviation, %
RSMD	Mean Square Deviation, %
h	height of the sun
d	Declination, degree
Tl	linke's disturbance factor
Ahe	winter-summer alternation
Z	altitude, km
I	irradiance, w/m^2
i	angle of incidence, degree
n	number of observations

Greek symbols

λ	longitude
β	angle of inclination of the receiving surface
γ	zenith angle
Ω	Hour angle
ϕ	Latitude
ρ	albedo

Subscripts

D, H	direct horizontal
d, H	diffuse horizontal
G, H	global horizontal
D,I	direct inclined
d,I	diffuse inclined
d, sky	diffuse from the sky
r	backscatter
re	reflection
d,ground	diffused on the ground
nor	normal
s	solar
e,i	estimated irradiance
m,i	measured irradiance
R	correlation coefficient